HHS Public Access

Author manuscript

Nat Neurosci. Author manuscript; available in PMC 2018 July 29.

Published in final edited form as:

Nat Neurosci. 2018 March ; 21(3): 404–414. doi:10.1038/s41593-018-0071-y.

Insular Cortex Mediates Approach and Avoidance Responses to Social Affective Stimuli

Morgan M. Rogers-Carter[1,2], **Juan A. Varela**[1,2], **Katherine B. Gribbons**[1], **Anne F. Pierce**[1], **Morgan T. McGoey**[1], **Maureen Ritchey**[1], and **John P. Christianson**[1,*]

[1]Department of Psychology, Boston College, Chestnut Hill, MA, USA

Abstract

Social animals detect the affective states of conspecifics and utilize this information to orchestrate social interactions. In a novel social affective preference text in which experimental adult male rats could interact with either naive or stressed conspecifics, the experimental rats either approached or avoided the stressed conspecific, depending upon the age of the conspecific. Specifically, experimental rats approached stressed juveniles but avoided stressed adults. Inhibition of insular cortex, which is implicated in social cognition, and blockade of insular oxytocin receptors disrupted the social affective behaviors. Oxytocin application increased intrinsic excitability and synaptic efficacy in acute insular cortex slices, and insular oxytocin administration recapitulated the behaviors observed toward stressed conspecifics. Network analysis of Fos immunoreactivity in 29 regions identified functional connectivity between insular cortex, prefrontal cortex, amygdala and the social decision-making network. These results implicate insular cortex as a key component in the circuit underlying age-dependent social responses to stressed conspecifics.

Keywords

insular cortex; rat; empathy; oxytocin; intrinsic excitability; affect; graph theory; social decision-making

INTRODUCTION

Social animals have an enormous repertoire of behavioral expressions that enable the transmission of affect to other members of the group[1]. Sensory and perceptive systems in the "social decision-making network" (SDMN) allow one to appraise these social stimuli and

[*]**Corresponding Author:** John P. Christianson, Department of Psychology, Boston College, Chestnut Hill, MA, USA, j.christianson@bc.edu, Phone: +1-617-552-3970.

[2]These authors made equal contributions to this work

Author Contributions

Conceptualization, J.P.C., J.A.V., M.M.R-C., M.R.; Methodology, M.M.R-C., J.A.V., M.R. J.P.C.; Investigation; J.A.V., M.M.R-C., K.B.G., A.P., M.M., M.R., J.P.C.; Writing – Original Draft, J.A.V., M.M.R-C., and J.P.C.; Writing -- Revision & Editing, M.M.R-C., M.R., J.P.C.; Funding Acquisition, J.P.C.; M.M.R-C.

Competing Financial Interests Statement

The authors declare no direct or indirect biomedical financial interests or other potential conflicts of interest.

integrate them with past experiences, situational, and somatic factors to shape specific social affective behavioral responses[2]. In addition to the SDMN, growing evidence implicates insular cortex in responding to social affective stimuli in humans. Specifically, emotion recognition and empathic deficits occur after insular cortex lesions[3–5], and empathic deficits in autism spectrum disorder (ASD) are related to insular cortex activity and connectivity[6–9].

The relationship between insular cortex and social affect in humans is likely a consequence of insular connectivity to sensory systems, which position it as locus of multisensory integration[10]. Importantly, insular cortex is interconnected with the SDMN; this connectivity includes inputs from the hypothalamus[11] and ventral tegmental area[12], reciprocal connections with the amygdala[13] and outputs to periaqueductal gray[14], bed nucleus of the stria terminalis, nucleus accumbens[15], and medial prefrontal cortex[16]. The insular cortex also receives input from oxytocin (OT)-containing axons from the paraventricular nucleus[17], and OT receptor (OTR) binding is enriched in the insular cortex[18]. OT modulates social behaviors across species[19], including empathic cognition in both humans[20] and rodents[21]. OT relieves social deficits observed in ASD and augments insular activity and connectivity[22,23], suggesting a mechanistic relationship between OT, insula and social cognition.

Translational rodent models that capture aspects of social affect include emotion contagion and social buffering[24]. However, some paradigms require learning or direct exposure to a conspecific in pain, making it difficult to isolate social affective processes from other motivations[21,25]. We developed a rat social affective preference (SAP) test in which social affective behaviors were objectively quantified as a preference to approach or avoid interaction with a conspecific that had received a mild stressor. Because the experimental rat in the SAP test was not exposed to, nor witness to, the stressor itself, the unconditioned behavior of the experimental subject toward the conspecifics can be interpreted as a response to the affective state of the conspecific. We report a set of *in vivo* and *in vitro* studies that implicate insular cortex activity and modulation by OT as necessary and sufficient for modulating social affective behaviors in rat. Graph-theory based network analyses[26] were performed to characterize, in rats, the relationship of the insular cortex to several regions of interest (ROIs) implicated in social decision making.

Results

Age and stress exposure of conspecific determine social approach

In the SAP test an experimentally naive, adult male rat was presented with a pair of unfamiliar conspecific male stimuli (see Fig. 1 and Supplementary Video 1). To manipulate social affect, one of the conspecifics was exposed to a mild stressor of 2, 5s 1mA footshocks immediately before the test, while the other did not receive footshocks (naive). Because social approach behaviors are shaped, in part, by features of the target including age[27], we hypothesized that the response of experimental rats to stressed conspecifics may depend on the conspecific's age. Twenty experimental adult male rats (PN 60–80 days) underwent SAP tests (Figs. 1A & 1B) in which the choice test involved exposure to a pair (one stressed, one naive) of unfamiliar male pre-pubertal juveniles or a pair of unfamiliar male adults[28]. The design was a 2 by 2 with conspecific Age (PN 30 vs. PN 50) as a between-subjects factor

and conspecific Affect (naive or stress) as a within-subjects factor. We observed an increase in social interaction with the stressed juvenile (Fig. 1C, $p < 0.0001$) but a decrease in interaction with the stressed adult ($p = 0.020$). To summarize this interaction, we computed a percent preference score by dividing the time spent interacting with the stressed conspecific by the total time spent interacting during the test (Fig. 1D). Analysis of *conspecific* behavior revealed that stress caused juvenile conspecifics to engage in more self-grooming compared to the naive juvenile conspecific, but stress did not influence any other conspecific behaviors (Sup. Fig. 1).

The SAP procedure was replicated several times in later optogenetic and pharmacology experiments, which provided a large sample to evaluate the reliability and generality of these phenomena, and to quantify changes in experimental adult rat behavior from the habituation day to the SAP test day. Data from SAP tests conducted under either vehicle, Light-OFF or sham treatments were pooled and converted to percent preference scores (Fig. 1E) and the scores were found to fit a normal distribution (D'Agostino and Pearson normality test, for PN 30: $K2 = 2.52$, $p = 0.284$, for PN 50: $K2 = 2.14$, $p = 0.343$). PN 30 and PN 50 preference scores to the hypothetical value of 50% (equal time exploring both naive and stressed conspecifics, on sample t-tests, 2-tailed) revealed a preference for the stressed PN 30 ($p < 0.0001$) and a preference for the naive PN 50 ($p < 0.0001$). Approximately 82% (42 of 51) of rats tested with PN 30 conspecifics exhibited a preference for the stressed target, while only 21% (10 of 46) of rats tested with PN 50 conspecifics exhibited preference for the stressed target. The same pattern was also observed in SAP tests with female experimental adults (Sup. Fig. 2). To evaluate whether exposure to the stressed conspecific in the SAP tests altered any other aspect of experimental adult behavior, we quantified behaviors of the experimental adult rats during habituation and SAP tests (Fig. 1F). While most behaviors measured were equal across tests, a significant Age by Behavior by Test (habituation vs. SAP) interaction ($p = 0.025$) reflected increases in arena investigation ($p = 0.05$) and self-grooming ($p = 0.035$) during SAP tests with PN 50 conspecifics.

From the SAP test results we predicted that in one-on-one interactions an experimental adult should engage in more social interaction when exposed to a stressed juvenile than when exposed to a naïve juvenile, and the opposite pattern for adult targets. Experimental adult rats were given a series of 2 "one-on-one" social exploration tests (5 min duration, one test per day) with 1 unfamiliar naive PN 30 juvenile followed by 1 unfamiliar stressed juvenile as the social interaction targets (Fig. 1G); a separate set of experimental adults received the same series of tests with PN 50 adult conspecifics. A within-subjects design was used with test order counterbalanced. As in the SAP test, experimental adults spent more time interacting with the stressed juvenile ($p = 0.0002$) and less time with the stressed adult ($p = 0.041$; Fig. 1H, and see Sup. Fig. 2 for a serial variation of this test). There was no difference in conspecific-initiated social investigation at either age.

Conspecific stress alters ultrasonic vocalizations

Ultrasonic vocalizations (USVs) signal emotional states in rats[29]. To explore whether stress altered USVs during social interactions, a separate set of rats was given a 5 min one-on-one social interaction in a chamber equipped with an ultrasonic microphone. Social interaction

and USVs were quantified during exposure to one of 4 conspecific stimuli: Naive PN 30, Naive PN 50, Stressed PN 30 or Stressed PN 50. Three types of vocalizations were present in our recordings: 22kHz flat vocalizations, ~30–60kHz rising calls, and ~60–80kHz trills (Fig. 1I and Sup. Fig. 3). Rising and Trill calls, which are emitted during and in anticipation of rewarding stimuli, were quite frequent during naive interactions but reduced during stressed interactions (Fig. 1J). 22kHz vocalizations are thought to convey negative affect, and these were observed primarily during interactions with stressed adults (Fig. 1K). More 22kHz calls were evident in interactions with PN 50 stressed rats than with PN 50 naive ($p = 0.0052$), PN 30 stressed ($p = 0.0070$) or PN 30 naive ($p < 0.0001$) rats; there were fewer rising calls in interactions with PN 30 or PN 50 stressed rats than with naive conspecifics ($p = 0.0446$ and $p < 0.0001$, respectively), more rising calls in interactions with stressed PN 30 rats than stressed PN 50 ($p = 0.0304$), fewer trills in interactions with PN 30 and PN 50 stressed rats than with naïve rats ($p < 0.0234$ and $p < 0.0001$, respectively) and a trend for more trills in the naive PN 50 compared to PN 30 ($p = 0.055$). Although it is impossible to determine whether stress reduced USVs emitted by conspecifics, by the experimental rat toward the stressed conspecific, or some combination of both, stressor exposure dramatically shifted the patterns of USVs consistent with a state of negative affect.

Optogenetic silencing of insular cortex prevented social affective preference

To test whether exposure to stressed conspecifics influences insular cortex activity, experimental rats were sacrificed 90 min after the one-on-one social interaction tests described for USV analysis and sections containing the insular cortex were stained for Fos immunoreactivity (Fig. 2A). Fos immunoreactivity was higher in the insula of rats that had interacted with stressed PN 30 conspecifics than in rats that had interacted with stressed PN 50 conspecifics (Fig. 2B, $p = 0.009$), and insula Fos immunoreactivity was lower in rats after interaction with PN 50 stressed rats than in rats after interaction with PN 50 naive rats ($p = 0.038$; pooled across region). A linear regression analysis with Age and Stress conditions included as moderators indicated that insula Fos levels predict social interaction ($p < 0.0001$, Fig. 2C). Together with a pilot study in which pharmacological inhibition of the insula prior to SAP tests altered the pattern of behavior observed in experimental rats (Sup. Fig. 4), these data suggest that the activity and, perhaps, output of the insular cortex are necessary for social affective behavior.

To inhibit insular cortex pyramidal neurons, experimental rats were transduced with halorhodopsin (AAV5-CamKIIα-eNpHR3.0-mCherry), which allowed reversible neuronal silencing (Fig. 2D, verification provided in Sup. Fig. 5). Two weeks after virus infusion, rats underwent SAP tests in a 2 Age (juvenile or adult conspecific) by 2 Affect (naive or stress) by 2 Light (OFF or light ON) design (Fig. 2E). Green light (ON) or no light (OFF) was delivered to the insula continuously during the SAP test. As expected, the majority of rats in the OFF condition exhibited preference for interacting with the stressed juvenile (9 of 12 experimental rats) and avoided the stressed adult (12 of 14 experimental rats), whereas experimental rats in the light ON condition avoided the stressed juvenile (Fig. 2F) or preferred interacting with the stressed adult (Fig. 2G; Age by Stress by Light interaction, $p < 0.0001$). The 5 rats that did not exhibit the expected preference pattern in light OFF were analyzed separately (Sup. Fig. 6). Pairwise comparisons in the juvenile + OFF condition

identified an increase in interaction with the stressed juvenile compared to naive juvenile (p = 0.0020), whereas in the adult + OFF condition there was a significant decrease in interaction with the stressed adult conspecific compared to the naive adult conspecific (p = 0.0121). In the light ON condition, there were no significant differences in exploration times with naive vs stressed conspecifics in either age condition (PN 30 p = 0.0722 and PN 50 p = 0.0625). Thus, silencing the insular cortex prevented the expression of social affective behaviors. Importantly, optical treatment had no effect on rats with sham transfections when interacting with PN 30 conspecifics (Fig. 2H), and did not influence exploratory activity or general behavior in the SAP test (Sup. Fig. 5).

Oxytocin alters the excitability of the insular cortex

The foregoing suggested that exposure to stressed conspecifics triggers a neurobiological response that alters insular cortex activity. Because OTRs are expressed in the insula and OT can modulate excitatory balance in cortical circuits[30], we hypothesized that OT could directly modulate insular cortex excitability. Active and passive intrinsic properties were characterized after bath application of OT (500nM) in whole-cell pyramidal neuron recordings (N = 27 neurons, Fig. 3). A complete list of parameters measured is provided in Table 1. OT caused depolarization of the resting membrane potential, an increase in input resistance, and a decrease in membrane time constant. These changes would permit the membrane to charge faster and reach the action potential threshold with less excitatory input. Indeed, OT also reduced the minimum current injection required to elicit an action potential (*i.e.* the rheobase) and reduced the slow after-hyperpolarization (sAHP). Together, these changes suggest that in the presence of OT, insular cortex pyramidal cells might achieve greater spike frequency. Consistently, spike frequency increased in response to sustained depolarizing currents. Interestingly, after OT application, action potentials were significantly smaller with decreased amplitude, rise rate, decay rate and longer duration (half-width), which may indicate that the increase in firing frequency could come at a cost of reduced neurotransmitter release. OTR is thought to signal through the $G\alpha_{q11}$ signaling cascade to raise intracellular Ca^{2+} levels and activate protein kinase c (PKC)[31]. To test whether the changes in intrinsic and synaptic physiology caused by OT were mediated by PKC, we applied the pan-PKC antagonist Gö 6983 (200nM) in whole-cell recordings with or without OT (500nM). Gö 6983 prevented the decrease in spike amplitude (Fig. 3F), increase in firing frequency (Fig. 3J) and increase in R_{input} (Fig. 3M) that were evident in OT-treated neurons.

To investigate the effect of OT on synaptic efficacy, input/output curves were conducted in acute insular cortex slices on a perforated 60 channel multiple electrode array (Fig. 4A–C). OT induced a leftward shift, with significantly larger fEPSP amplitude compared to baseline at stimuli from 2 to 5V with washout levels differing from OT beginning at 3V (ps < 0.0001). In the aCSF control slices synaptic responses were stable across all phases of the experiment. In the presence of Gö 6983 (200nM), OT (1μM) did not alter fEPSP input/output curves (Fig. 4G–H). Thus, OT augmented evoked excitatory synaptic transmission.

An increase in intrinsic excitability might also be reflected in a change in the miniature and/or spontaneous release of excitatory neurotransmitter in the slice. We made continuous whole-cell, voltage-clamp recordings of deep layer insular cortex pyramidal neurons (N =

19) before and after application of OT (500nM) to quantify miniature excitatory postsynaptic currents (mEPSCs, Fig. 4D–F). OT reduced mEPSC amplitude ($p = 0.004$) but had no effect on mEPSC frequency. Taken together, the electrophysiology data suggests that OT rendered insular cortex pyramidal neurons more responsive to excitatory inputs via activation of PKC second messenger cascades.

Insular cortex oxytocin receptors are necessary for both prosocial and asocial responses to stressed conspecifics

We next determined whether insular cortex OTRs contribute to the prosocial or asocial behaviors in the SAP test. Experimental rats (N = 20) were implanted with bilateral cannula guides to the insular cortex. Rats underwent the SAP procedure in a 2 by 2 by 2 experimental design with conspecific Age (PN 30 vs. PN 50) as a between-subjects factor, and with Drug (Vehicle or OTRa 20ng/side) and conspecific Stress as within-subjects factors (Fig. 5A). The rats received microinjections 15 min before SAP tests on days 3 and 4, with drug order counterbalanced. The conspecific stimuli were always unfamiliar; no effect of test order was apparent. Two subjects in the PN 50 condition with misplaced cannula were excluded (Sup. Fig. 6). In the vehicle condition, 7 of 10 experimental rats exhibited a preference for stressed over naive juveniles and 7 of the 8 experimental rats exhibited a preference for naive over stressed adults (Fig. 5B–C). Rats that did not exhibit preference in the vehicle condition were analyzed separately (Sup. Fig. 6). There was a significant Age by Drug by Affect interaction ($p < 0.0001$), with greater time spent investigating the stressed PN 30 conspecific (vs. the naive PN30) and less time investigating the stressed PN 50 conspecific (vs. the naïve PN50) in the vehicle conditions ($ps = 0.001$), but more time interacting with the naive PN 30 conspecific ($p = 0.06$) and less time with the naive PN 50 conspecific ($p = 0.014$) in the OTRa condition. Percent preference scores revealed an Age by Drug interaction ($p < 0.0001$), with opposing effects of OTRa in experimental rats' behavior towards PN 30 ($p = 0.011$) and PN 50 ($p = 0.002$) groups. Thus, blockade of insular cortex OTRs prevented the age-dependent approach and avoidance behavior in response to stressed conspecifics in the SAP test.

A separate set of rats (N = 16) was prepared with bilateral insular cannula as above and underwent one-on-one interactions with either a stressed PN 30 juvenile or a stressed PN 50 adult conspecific (between-subjects) 15 min after vehicle or OTRa injections (within-subjects) in a 2 by 2 design; drug order was counterbalanced by day as above (Fig. 5D). One experimental rat interacting with adult conspecifics had a misplaced cannula and was excluded. ANOVA revealed a main effect of Age and Age by Drug interaction ($ps < 0.0001$). The main effect of age indicates more interaction time with the stressed juveniles than the stressed adults. OTRa microinjection reduced the time spent interacting with the stressed PN 30 conspecifics ($p = 0.0008$) and increased the time interacting with stressed PN 50 conspecifics ($p = 0.009$) in the one-on-one tests (Fig. 5E).

Insular cortex oxytocin administration recapitulates social affective behaviors toward naive conspecifics

We next determined whether intra-insular OT administration was sufficient to increase or decrease experimental rat interaction with non-stressed PN 30 or PN 50 conspecifics,

respectively. Bilateral insular cannula implants were made in 32 rats and after recovery each received 2 one-on-one social interaction tests (3 min duration) with unfamiliar naive PN 30 or PN 50 conspecifics. A within-subjects design was used such that each rat received vehicle injections prior to one test and OT (250 pg/side; equivalent to 500nM) before the other. Injections were made 15 min before testing and drug treatment order was counterbalanced. One rat from each age group did not receive injections and was removed from analysis. OT increased time spent interacting with the naive PN 30 conspecific ($p < 0.0005$) and decreased time with the naive PN 50 conspecific ($p = 0.002$, Fig. 5F).

Social responses to stressed conspecifics require insular cortex protein kinase C (PKC)

The foregoing suggested the possibility that behavioral responses to stressed conspecifics depend upon modulation of intrinsic excitably in the insular cortex by OT and so we predicted that interference with insular cortex PKC would mimic the effect of OTRa. Rats received bilateral insular cortex cannula implants and underwent SAP tests with pretreatment with either vehicle or Gö 6983. Eight of 10 rats exhibited preference for the stressed PN 30 conspecific after vehicle injection and 7 of 11 rats avoided the stressed PN 50 conspecific (Fig. 5G). In these rats, Gö 6983 reversed the pattern observed under vehicle (Age by Stress by Drug interaction, $p < 0.0001$). In tests with PN 30 conspecifics, experimental rats spent more time interacting with the stressed than naive conspecifics after vehicle injection ($p < 0.0001$) and less time interacting with the stressed than naive conspecific after Gö injection ($p = 0.0090$). In tests with PN 50 conspecifics, the experimental rats spent less time interacting with the stressed conspecific in the vehicle condition ($p = 0.0057$) but equal time interacting with the stressed conspecific after Gö injection ($p = 0.1614$). To summarize the behavioral studies, experimental adult rats preferred to interact with stressed juveniles but avoided interaction with stressed adult conspecifics. In the insular cortex, optogenetic silencing, blockade of the OTR, and inhibition of PKC each interfered with experimental rat responses to stressed conspecifics and OT administration was sufficient to reproduce the phenomena with naive conspecifics.

Insular cortex and the social decision-making network

The insular cortex is anatomically connected to the SDMN, prefrontal cortex and amygdala. We assessed insular functional connectivity using Fos analysis in 29 ROIs spanning the insular cortex, prefrontal cortex, extended amygdala and the SDMN (Sup. Table 1, and Sup. Fig. 7) in the 44 rats that were used for USV analysis. A data-driven community detection analysis revealed a network with 2 modules (Fig. 6A), in which ROIs were more highly correlated within each module than between modules (maximized modularity quotient = . 59). The degree to which ROI Fos levels were correlated within and between modules varied across the groups, with generally stronger correlations in the stressed juvenile condition (Fig. 6B). The 2 modules contain ROIs that may be categorized generally as “social” (green module) and “emotional” areas (purple module), respectively (Fig. 6C). We evaluated the participation coefficient for each node (Fig. 6D, Sup. Fig. 8); this is a measure of the degree to which nodes correlate with multiple modules and has been argued to be an appropriate measure of “hubness” for correlation-based networks[32]. Agranular insular (AI) cortex was among the nodes with the highest participation coefficients along with prelimbic prefrontal cortex, piriform cortex and dorsal bed nucleus — regions that are associated with emotion

contagion[33], social learning[34] and as a hub in the SDMN[2], respectively. Thus, data-driven network analyses revealed functional integration among regions in the social brain, and suggest that the insula is positioned to interact with previously identified nodes important for social and affective behaviors.

DISCUSSION

To better understand the neural basis of social affective behavior, we developed a social affective preference (SAP) test in which the choice to approach or avoid a stressed conspecific could be quantified. In the SAP test, behaviors depended upon both the age and emotional state of the conspecific, which may reflect a species-specific adaptation in which social stress signals are danger cues when generated by an adult, but prosocial cues when generated by juveniles. *In vivo* pharmacological experiments, *in vitro* studies and network analyses suggest that exposure to a stressed conspecific evokes OT release within the insular cortex which, via modulation of insular cortex output neuron excitability, orchestrates species-specific, age-dependent approach or avoidance behaviors via modulation of the social decision-making network (SDMN). The findings provide new insight into the neural basis of elementary social affective processes and, consistent with human neuroimaging work, warrant consideration of the insular cortex as an important component of the social brain.

A central ideal in social neuroscience is that social behaviors involve the integration of multisensory cues with situational and somatic factors[35]. In rodents, social communication of emotion occurs via chemosignals[36], vocalizations[29], and overt behaviors[37]. Foot-shocked rats emit social odors that can either attract conspecifics in social buffering or serve as social alarm signals[38]. Although we did not investigate chemosignals, these likely contribute to the behavior of the experimental rats in the SAP test. Regarding vocalizations, 22kHz USVs are emitted as alarm signals, and frequency modulating USVs are thought to convey positive affect[39]. Accordingly, 22kHz vocalizations were nearly undetectable during naive-naive interactions, but increased dramatically when one of the conspecifics was a stressed adult. Frequency modulating (rising and trill) calls preceded bouts of social interaction (Sup. Fig. 3) and were abundant in naive-naive interactions but dropped considerably when one of the conspecifics had received footshock, a pattern consistent with a negative affective state in the stressed conspecifics. Regarding overt behaviors, stress increased the amount of time juvenile conspecifics engaged in self-grooming. Thus, the experimental rat may draw from vocalizations, visible cues and chemical signals to compute the age and emotional state of the conspecific. Suitably, the piriform cortex and medial amygdala Fos, key olfactory processing areas modulated by OT during social interactions[40], were found among the highest participation coefficients in the network analysis (Fig. 6D, Sup. Fig. 8). Additional studies are needed to establish which stimuli emitted by stressed conspecifics determine social affective behaviors and how this information converges on the insular cortex.

The decision to avoid a stressed adult may be adaptive as the stressed conspecific may be perceived as a social danger cue. On the other hand, it is difficult to pinpoint the motivation to approach the stressed juvenile. In human social behavior, features of the target stimulus, including age, are critical determinants of whether or not someone will approach, help or

avoid another in distress[27], and there are examples of prosocial responses to stressed conspecifics in both voles[21] and mice[41]. These prosocial examples appear to have boundary conditions. First, prosocial effects are evident in pair-bonded voles and familiar female mice, but not between strangers or in male mice; this may also generalize to rats[42] (but see[25]). An effect of the conspecific's age has not previously been investigated, and our results suggest that prosocial behaviors may occur towards unfamiliar conspecifics if they are juveniles, regardless of sex (Sup. Fig. 2). Regardless of the motivation underlying the behavior of experimental rats in response to stressed conspecifics, the phenomenon reported here is direct evidence of what de Waal argued to be the most elementary component of empathy: "that one party is affected by another's emotional or arousal state (p. 282)."[43] The SAP test may provide a useful addition to the preclinical toolkit for investigating psychiatric diseases in which social behavior is impaired, such as autism and schizophrenia.

Insular cortex is positioned to integrate social affective stimuli as a nexus between multimodal sensory inputs and emotional, executive, and social circuits in the limbic system[10]. Analysis of Fos immunoreactivity across ROIs representing these systems revealed several features of the network underlying social affective behavior. Highly correlated patterns of activity emerged in 2 modules (Fig. 6) which were composed primarily of structures found in the SDMN or the structures associated with emotion, such as the nuclei of the extended amygdala and prefrontal cortex. Insular cortex subfields were found in both of these modules with a high degree of participation in both networks suggesting, together with the established anatomical connectivity, that it may integrate social and emotional processes. These features may be key to understanding why inhibition of the insular cortex not only interfered with social affective preferences, but in fact reversed them (Sup. Fig. 9). We hypothesize that exposure to stressed conspecifics elicits parallel activity within these modules which compete for control to either approach or avoid. OT altered several properties of insular neurons that are consistent with such a modulatory role, namely a reduction in AP amplitude, increase in R_{input}, increase in input/output relationships, reduction in sAHP and potentiation of evoked insular fEPSCs. Indeed, OT can increase spike output *in vivo*[44] and our data suggest an intrinsic mechanism that may underlie shifts in synaptic efficacy and excitatory/inhibitory balance found in cortical regions where OT is critical for myriad social behaviors[30,34]. Thus, in concert with sensory cues that identify the age of the conspecific, OT may bias the output of insula efferents to the ventral striatum or prefrontal cortex to promote interaction with stressed juveniles, or to the basolateral amygdala to promote avoidance in response to stressed adults as these are thought to be the proximal mediators of the rewarding, empathic, and emotional aspects of social behavior, respectively[45].

Like social behavior itself, the effects of OT administration on social decision-making are sensitive to situational and interpersonal factors, with OT sometimes producing prosocial effects and at other times anti-social effects[46]; both were observed after insular OT administration. Abnormalities in emotion recognition are central to several psychiatric conditions including ASD[47,48], in which OTR polymorphisms[49,50] and insular cortex hypofunction[8,9] are correlates of symptom severity. Our results suggest that disruption of insula function may be key to pathophysiology in behaviors that depend upon social decisions regarding the emotions of others. The SAP test and the network model of insular

input to the SDMN presented here provide a platform for further research into the neuroanatomical and physiological systems that integrate social information with decision-making and behavior.

ONLINE METHODS

Rats

Male and female Sprague-Dawley rats were obtained from Charles River Laboratories (Wilmington, MA). Rats were allowed a minimum of 7 days to acclimate to the vivarium after arrival and housed in groups of 2–3 with free access to food and water on a 12 h light/dark cycle. Behavioral procedures were conducted within the first 4 h of the light phase. All reagents and chemicals were purchased from Fisher Scientific, Tocris or Sigma unless otherwise noted. All procedures were conducted in accordance with the Public Health Service *Guide for the Care and Use of Laboratory Animals* and were approved by the Boston College Institutional Animal Care and Use Committee.

Social Affective Preference (SAP) Test

The SAP test allowed quantification of social interactions initiated by an adult test rat when presented simultaneously with two unfamiliar conspecific stimuli. To begin the test, the adult test subject was placed into a clear plastic cage (50 × 40 × 20 cm, L × W × H) with a wire lid. Pairs of stimuli rats were either juvenile (PN 30 +/− 2 days old) or adult (PN 50 +/− 2 days old) and were placed inside one of two clear acrylic plastic enclosures (18 × 21 × 10 cm, L × W × H) on either end of the arena. Interaction between the experimental and stimuli rats was permitted on one side of the enclosure, which consisted of clear acrylic rods, spaced 1 cm center-to-center (see photo, Fig. 1) and as in[52]. To habituate subjects to the procedure on days 1 and 2 the adult was placed in the arena for 60 min and then empty enclosures (Day 1) or enclosures containing experimentally naive, unfamiliar stimuli (Day 2) were added for 5 min. To assess social affective preference, on Day 3 two unfamiliar stimuli were added, but one of the stimuli rats was exposed to 2 footshocks (1mA, 5 sec duration, 60 sec inter-shock-interval, Precision Regulated Animal Shocker, Coulbourn Instruments, Whitehall, PA) immediately prior to the 5 min test to induce a stressed affective state. Shock occurred in a separate room and shock parameters were selected because they were sufficient to produce a conditioned fear in our laboratory (data not shown). The 5 min test length was selected after pilot studies in which we observed a reliable decrease in social behavior after the first 5 min of test. In experiments involving optogenetics or intracerebral injections, a within-subjects design was employed such that each adult test subject was exposed to both vehicle and experimental treatments in SAP tests on consecutive days. A trained observer quantified the time spent in social interaction with each of the stimuli. Social interaction consisted of nose-nose and nose-body sniffing, and reaching into the enclosure to contact the stimulus rat. Digital video recordings were made of each test for later determination of inter-rater-reliability by a second observer completely blind to the experimental manipulations and hypotheses. Across the experiments included in this report we observed very high inter-rater reliability, $t(80) = 0.966$, $r^2 = 0.93$, $p < 0.0001$. Although conceived independently, this paradigm has a number of features in common with the method recently reported with voles[53]. For some tests, we also quantified a number of behaviors in the experimental adult

rat from videos including time spent 1) sniffing or investigating the test arena, 2) immobile, 3) digging in the bedding, 4) self-grooming, and 5) biting or pulling at the conspecific. Videos were selected blind to SAP test social interaction results. The first three measures were assessed to quantify general locomotor activity, self-grooming has been argued to reflect emotion contagion[21] and biting may reflect aggressive behaviors.

One-on-One Social Exploration Tests

As previously[54] each experimental subject was placed into a plastic cage with shaved wood bedding and a wire lid 60 min before the test. To begin the test a juvenile or adult was introduced to the cage for 5 min and exploratory behaviors (sniffing, pinning, and allogrooming) initiated by the adult test subject were timed by an observer blind to treatment. Juvenile and adult stimuli rats were used for multiple tests but were never used more than once for the same adult test rat. Each experimental adult was given tests on consecutive days once with an unfamiliar naive conspecific and once with an unfamiliar stressed conspecific (2 foot shocks, exactly as above); test order was counterbalanced.

Insular Cortex Cannula Placement and Microinjection

Under inhaled isoflurane anesthesia (2–5% v/v in O_2), cannula (26g, Plastics One, Roanoke, VA) were inserted bilaterally into the insular cortex (from Bregma: AP: −1.8mm, ML: +/−6.5mm, DV: −6.2mm from skull surface) and fixed in place with acrylic cement and stainless steel screws. Rat were administered the analgesic meloxicam (1mg/kg, Eloxiject, Henry Schein) and antibiotic penicillin G (12,000 Units, Combi-pen 48, Henry Schein) after surgery and allowed between 7–10 days recovery prior to experimentation. The OTR antagonist (OTRa) desGly-NH_2-d$(CH_2)_5$[Tyr(Me)^2,Thr^{4}OVT[55] as in[56] and OT were dissolved in sterile 0.9% saline vehicle, the pan-PKC inhibitor Gö 6983 was first dissolved in 100% DMSO and then diluted to 200nM in a vehicle of 10% DMSO and water. All injections were 0.5μL per side and infused at a rate of 1μL/min with an additional minute for diffusion. At the conclusion of the experiment, rats were overdosed with tribromoethanol (Sigma) and brains were dissected and sectioned at 40 μm to verify the microinjector tip location using cresyl violet stain and comparison to stereotaxic atlas[51]. Rats with occluded injectors or having cannula located outside of the insular cortex were excluded from all analyses (See Supplementary Fig. 6). To control for nonspecific effects of OTRa on social behavior we conducted a control experiment in which OTRa had no effect on interaction between experimentally naive adult and PN 30 rats (Sup. Fig. 10).

Optogenetics

Adult male rats underwent stereotaxic surgery to be implanted with bilateral guide cannula designed to fit a 200um optical fiber (Plastics One). After the cannula was secured, 250nL of a viral vector containing the neuronal silencing halorhodopsin eNpHr3.0 under the CamKIIα promoter (AAV5-CamKIIα-eNpHR3.0-mcherry)[57] or a sham virus (AAV5-CamKIIα-YFP) was microinjected at a depth 1mm below the termination of the guide cannula at a rate of 50nL/min and allowed 5 min for diffusion. Optogenetic transductions were evaluated by fluorescence microscopy and *in vitro* whole cell recordings (Supplementary Fig. 5). During testing, a multimodal fiber optic wire (200um core, 0.39NA, Model FT200EMT, Thorlabs) extending 1mm below the cannula tip was affixed to the stylet

via a screw top ferrule (Plastics One) and connected to a laser (GL523T3-100, Shanghai Laser & Optics Century). Throughout the length of a social test green light (λ = 523nm) at a power of ~10–15mW/mm^2 was administered to maintain insular inhibition for the light ON conditions. During the light OFF condition, rats underwent the social test while connected to the laser but no light was administered. Functional photo inhibition was verified in whole cell recordings of mCherry positive insular cortex pyramidal neurons in acute brain slices before, during, after green light administration (10mW/mm2) delivered through the objective of the electrophysiology microscope. The extent of transfections was determined by imaging mCherry expression with widefield fluorescent microscopy (Zeiss AxioImager Z2). Locations of transfections are provided in Supplementary Figures 5 and 6.

Electrophysiology Solutions and Drugs

All chemicals were purchased from Fisher Scientific, Sigma-Aldrich or Tocris. Standard artificial cerebrospinal fluid (aCSF) and recording solutions were used[58]. aCSF recording composition was (in mM) NaCl 125, KCl 2.5, $NaHCO_3$ 25, NaH_2PO_4 1.25, $MgCl_2$ 1, $CaCl_2$ 2 and Glucose 10; pH = 7.40; 310 mOsm; aCSF cutting solution was: Sucrose 75, NaCl 87, KCl 2.5, $NaHCO_3$ 25, NaH_2PO_4 1.25, $MgCl_2$ 7, $CaCl_2$ 0.5, Glucose 25 and Kynureinic acid 1; pH=7.40, 312 mOsm. The internal recording solution consisted of (in mM) K^+-Gluconate: 115, KCl 20, HEPES 10, Mg-ATP 2, Na-GTP 0.3, and Na-Phosphocreatine 10. pH = 7.30; 278 mOsm with 0.1% biocytin. Kynurenic acid 1 mM and SR-95531 2 μM were always added to the recording aCSF to block synaptic transmission for intrinsic recordings.

Insular cortex slices

Adult male rats were anesthetized with isofluorane, intracardially perfused with chilled (4°C), oxygenated aCSF cutting solution and quickly decapitated. 300 μm coronal slices including the insular cortex were taken using a vibratome (VT-1000S, Leica Microsystems, Nussloch, Germany). The slices were placed in oxygenated aCSF cutting solution (95% O^2 and 5% CO^2) at 37°C for 30 min and then at room temperature for a minimum of 30 min before slices were used for electrophysiological recordings.

Electrophysiology

Whole-cell current-clamp recordings were obtained at 30 ± 2°C. Patch-clamp electrodes were pulled (P-1000, Sutter Instruments, CA) from 1.5 mm outer diameter borosilicate glass (Sutter Instruments, CA) and filled with intracellular solution. Electrode resistance was 3–5 MΩ in the bath and recordings were only included if the series resistance remained less than 30 MΩ with less than 10% change from baseline throughout the experiment. Slices were visualized using a 40× (0.75 NA) water immersion objective under infrared differential interference contrast imaging on an upright microscope (AxioExaminer D1, Zeiss, Germany). All recordings were obtained with an Axon 700B amplifier and pClamp 10 (Molecular Devices), using appropriate bridge balance and electrode-capacitance compensation. After achieving a whole-cell configuration, baseline recordings were made in aCSF until 10 minutes of stable baseline were observed, at which point 500 nM oxytocin citrate was added to the bath. The dose of 500 nM was selected after a pilot study using a range of doses from 50nM to 1μM, the largest dose reported[59]. Because OT has high affinity for the Vasopressin 1A receptor (V1a), experiments typically isolate effects of OT to the

OTR by using synthetic OTR agonists or a cocktail of OT and V1a antagonists. These steps were not taken here because although V1a receptor mRNA has been reported throughout cortex[60] V1a receptor binding is not evident in adult male rat insula[61]. Analyses were performed using custom software written for Igor Pro (Wavemetrics Inc., Lake Oswego, OR).

As previously[62], active properties were quantified from single spikes by holding the neuron at −67 mV, and 2.5 ms current pulses were injected to elicit a single AP. Passive properties were measured by holding the membrane potential at −67 mV and injecting 1 s current pulses through the patch electrode. The amplitudes of the current injections were between −300 pA and +400 pA in 50 pA steps. All traces in which APs were elicited were used to generate input-output curves as the total number of APs per second plotted against the injected current. EPSCs were made in the whole cell configuration with the same internal solution and aCSF with tetrodotoxin (1uM) added to some of the recordings (7 of 19 total cells) to isolate miniature EPSCs. However, in our recording conditions very few large events, indicative of spontaneous glutamate release, occurred, so all events were assumed to be miniature EPSCs (mEPSCs) and the data were pooled (N = 19). Recordings were made for 10 min prior to OT (10 min) and then for 10 min after OT. mEPSC frequency and amplitude were determined with the mini analysis program (Synaptosoft). After recording, the slice was fixed in 4% paraformaldehyde and biocytin was visualized using the ABC method and NovaRed (Vector labs, Burlingame, CA). Only neurons with a pyramidal morphology and soma in deep layers of insular cortex were included for analysis. In a pilot experiment, no effect of OT was found on spontaneous inhibitory post-synaptic potentials (data not shown). The change in mEPSC amplitude observed likely reflects a postsynaptic modulation of AMPA receptor mediated currents[63] but not an effect of OT on the spontaneous circuit activity *per se.* However, OT did not influence AMPA:NMDA current ratio (data not shown).

Evoked field excitatory postsynaptic potentials (fEPSPs) were recorded on a 6 × 10 perforated multiple electrode array (Model: MCSMEA-S4-GR, Multichannel Systems) with integrated acquisition hardware (Model: MCSUSB60) and analyzed with MC_Rack Software (Version 3.9). Slices were placed on the array and adhered by suction of the perfusion through the perforated substrate. Bath solutions were as above and perfused through the slice from above. A stimulating electrode was selected in the deep layers of insular cortex, and fEPSPs were recorded after stimulation (0 to 5V, biphasic 220us, 500mV increments) before, during application of 500nM OT, and after (Wash). Each step in the I/O curve was repeated 3 times (20s inter-stimulus-interval) and each family of steps was replicated 3 times in each phase of the experiment. fEPSPs from channels displaying clear synaptic responses (as in Fig. 4B) and in the vicinity of the stimulating electrode were normalized to the individual channel's maximum response to 5V stimulation at baseline; channels from the same slice were averaged for group analysis.

The electrophysiology experiments were replicated to test the dependence of OT effects on PKC. A few key aspects of the experiments were different. First, a between-groups design was used such that baseline measures were taken from all neurons after a stable recording was achieved. Then, drugs were bath applied in aCSF that contained 0.5% DMSO to permit

solubility of the pan-PKC inhibitor Gö 6983 (200nM)[64]. The conditions were as follows: aCSF, aCSF with Gö 6983, OT (500nM for whole cell recordings, 1μM for fEPSPs), or OT with Gö 6983. The OT dose was increased to 1μM in the fEPSP experiment as 500nM did not reliably replicate the increase in fEPSPs when DMSO was added to the aCSF. All dependent measures were normalized to pre-drug baselines for analysis.

Ultrasonic Vocalization Recordings and Analysis

44 adult male rats were habituated for 1h to the test arena and 24h later randomly assigned to one of 4 treatment conditions: Naive-Juvenile, Naive-Adult, Stressed-Juvenile or Stressed-Adult in a 2 by 2 (Stress by Age) design (n = 11/group). Rats were given 5 min, one on one social interaction tests as above with conspecifics according to their treatment group. To record USVs, an acrylic lid was placed over the arena with a 192kHz USB microphone (Ultramic192K, www.Dodotronic.com) placed directly in the center. Recordings were made using Audacity 2.1 (www.audacityteam.org), exported as .wav files and audio spectrograms were generated in Raven Pro 1.5 (The Cornell Lab of Ornithology https://store.birds.cornell.edu/Raven_Pro_p/ravenpro.htm). USVs were identified using the Band Limited Energy Detector function within Raven Pro. High frequency “Trill” calls were found in the range of 8–20ms, from 55–80kHz; frequency modulating “Rising” calls were 30–100ms, from 35–68kHz; and 22kHz “flat” calls were greater than 100ms, from 18–28kHz. These ranges were drawn from the literature[29] and detection parameters were refined for each recording based on visual inspection by a trained observer who was blind to treatment condition.

Fos analysis

After testing for USVs, each rat was left in the test cage alone and placed in a quiet room for 90 min at which point the rat was overdosed with tribromoethanol and perfused with 0.01M ice-cold heparinized phosphate buffered saline (PBS) followed by 4% paraformaldehyde for later Fos analysis as previously reported[54]. Brains were dissected and post-fixed in 4% paraformaldehyde at 4°C for 24h and transferred to 30% sucrose for 2 days. 40μm coronal slices of the entire rostral-caudal extent of the brain were collected via a cryostat at −19°C and stored in 24-well plates containing cryoprotectant at 4°C. To visualize Fos, floating sections quenched for endogenous peroxidase with 3% H_20_2, blocked with 2% normal donkey serum in PBS-T (0.01% Triton-X100), and then incubated overnight in rabbit anti-c-fos antibody (1:500, Cat. No. sc-52, Santa Cruz). Sections were then washed and incubated in biotinylated donkey anti-rabbit secondary antibody (1:200, Cat. No. 711-065-152, Jackson ImmunoResearch) using the avidin-biotin complex method (ABC Elite Kit, Cat. No. PK-6100, Vector Labs) with chromogen precipitate (NovaRed Kit, Cat. No. SK-4800, Vector Laboratories). Sections were floated onto glass slides, dehydrated, cleared, and coverslipped with Permount. All steps were conducted at room temperature. To quantify Fos immunoreactive nuclei, tissue was imaged on a Zeiss Axioimager Z2 light microscope in the Boston College Imaging Core. Tiled images containing the ROIs were taken using a Zeiss AxioCam HRc digital camera through a 10× objective (N.A. 0.45). Representative images are provided in Supplementary Figure 7. Using ImageJ software, images were converted to 16-bit, ROIs were traced with reference to the rat brain atlas, and Fos immunoreactivity was quantified using the cell counter plug-in using parameters that were validated by comparison

to manual counts by a trained observer. Cell density was computed the number of Fos immunoreactive cells divided by the ROI area (in pixels) for ANOVA and network analyses.

Statistical Analysis

Sample sizes were initially determined based on prior work using social interaction[54,65] and intrinsic physiology[62], no formal statistical methods were used to pre-determine sample sizes. In all behavioral experiments, rats were randomly assigned to treatments. In electrophysiology experiments, cells were treated according to a Latin square design to achieve even representation of cells in treatment groups from different donor rats. For all of the experiments that entailed a mechanistic manipulation of the insular cortex including optogenetics, OT, OTRa, and PKC inhibitor infusions, we observed a portion of rats that did not exhibit the expected behavior towards stress conspecifics. Therefore, rats were excluded from the statistical analysis if any of the following conditions were met: 1) they did not express the expected preference for stressed juveniles or avoidance of stressed adults was greater or less than 50% in the control condition, 2) the cannula were occluded or found to be outside of the insula, and/or 3) virus expression was found to be unilateral or outside of the insula. The data from rats excluded due to item 1 above are provided for inspection in Supplementary Figure 6. To compare differences between mean scores of social interaction and electrophysiological endpoints we used t-tests and analysis of variance (ANOVA). Individual replicate data are provided in the figures. In most experiments, there were within-subjects variables, which were treated as such in the analysis (paired samples t-test or repeated measures ANOVA). The data distributions were visually inspected (all replicates are shown) and appeared to meet the assumptions for normality and equal variance; but these were not tested formally. Data were collected by observers blind to treatment. Final data analyses were not performed blind to the conditions of the experiments. Main effects and interactions were deemed significant when $p < 0.05$ and all reported post hoc test p values are Sidak-adjusted, to maintain an experiment-wise risk of type I errors at $\alpha = 0.05$. ANOVA analyses were conducted in Prism 7.0c (GraphPad Software) and SPSS Statistics 24 (IBM). A Life Sciences Reporting Summary is included in the online version of this manuscript.

Graph theoretical analysis has been applied to Fos datasets to characterize functional relationships in rodent neural circuits[66–69]. Network analyses were conducted with the Rubinov & Sporns (2010) Brain Connectivity Toolbox (https://sites.google.com/site/bctnet/) in MATLAB R2015a (The Mathworks Inc.). We conducted a graph theoretical analysis upon the Fos counts pooled across all treatment conditions to maximize network variation and to characterize the relationships among the ROIs, in which ROIs served as nodes and the rank-order correlations of Fos levels served as edges. Kendall's rank correlation was used to evaluate the relationships between each pair of the 29 included ROIs (nodes), computed across the sample of 44 rats that were used for USV analysis. Community detection analyses used a spectral community detection algorithm[70] applied to the weighted, unthresholded correlation network. Participation coefficients were calculated to determine the degree to which nodes participated in multiple networks, based on arguments that this measure is the most appropriate way to identify "hubs" in correlation-based networks[32]. Participation coefficients were based on positive edges only; additional network parameters are reported

in Sup. Fig. 8. Network visualization was conducted in R version 3.2.4 with the ggplot2[71] and ggnet[72] packages.

Code Availability

Network analysis scripts are freely available at https://github.com/ritcheym. Igor scripts are available from the corresponding author upon reasonable request.

Data Availability

The data that support the findings of this study are available from the corresponding author upon reasonable request.

Supplementary Material

Refer to Web version on PubMed Central for supplementary material.

Acknowledgments

The authors wish to thank Dr. M. Manning for kindly providing OTRa (University of Toledo), Dr. K. Deisseroth (Stanford University) for making optogenetic vectors freely available, and Drs. A. Veenema and D. Adams for constructive discussions related to the project. Funding for this work was provided by the Boston College Undergraduate Research Fellowships; National Science Foundation Grant #1258923 to M.M.R-C; NIH Grants MH103401 to M.R., MH093412, and MH109545 to J.P.C.; and the Brain and Behavior Research Foundation grant No. 19417 to J.P.C.

References

1. Darwin C. The expression of the emotions in man and animals Friedmann Julian, editorSt. Martin's Press; London: New York: 1976
2. O'Connell LA, Hofmann HA. The vertebrate mesolimbic reward system and social behavior network: a comparative synthesis. J Comp Neurol. 2011; 519:3599–3639. DOI: 10.1002/cne.22735 [PubMed: 21800319]
3. Gu X, et al. Anterior insular cortex is necessary for empathetic pain perception. Brain. 2012; 135:2726–2735. DOI: 10.1093/brain/aws199 [PubMed: 22961548]
4. Ibañez A, Gleichgerrcht E, Manes F. Clinical effects of insular damage in humans. Brain Struct Funct. 2010; 214:397–410. DOI: 10.1007/s00429-010-0256-y [PubMed: 20512375]
5. Leigh R, et al. Acute lesions that impair affective empathy. Brain. 2013; 136:2539–2549. DOI: 10.1093/brain/awt177 [PubMed: 23824490]
6. Blanken LM, et al. Cortical morphology in 6- to 10-year old children with autistic traits: a population-based neuroimaging study. Am J Psychiatry. 2015; 172:479–486. DOI: 10.1176/appi.ajp.2014.14040482 [PubMed: 25585034]
7. Di Martino A, et al. Relationship between cingulo-insular functional connectivity and autistic traits in neurotypical adults. Am J Psychiatry. 2009; 166:891–899. DOI: 10.1176/appi.ajp.2009.08121894 [PubMed: 19605539]
8. Morita T, et al. Emotional responses associated with self-face processing in individuals with autism spectrum disorders: an fMRI study. Soc Neurosci. 2012; 7:223–239. DOI: 10.1080/17470919.2011.598945 [PubMed: 21936743]
9. Odriozola P, et al. Insula response and connectivity during social and non-social attention in children with autism. Soc Cogn Affect Neurosci. 2015; doi: 10.1093/scan/nsv126
10. Gogolla N. The insular cortex. Curr Biol. 2017; 27:R580–R586. DOI: 10.1016/j.cub.2017.05.010 [PubMed: 28633023]

11. Allen GV, Cechetto DF. Functional and anatomical organization of cardiovascular pressor and depressor sites in the lateral hypothalamic area. II. Ascending projections. J Comp Neurol. 1993; 330:421–438. DOI: 10.1002/cne.903300310 [PubMed: 7682225]
12. Ohara PT, et al. Dopaminergic input to GABAergic neurons in the rostral agranular insular cortex of the rat. J Neurocytol. 2003; 32:131–141. [PubMed: 14707548]
13. Shi CJ, Cassell MD. Cortical, thalamic, and amygdaloid connections of the anterior and posterior insular cortices. J Comp Neurol. 1998; 399:440–468. [PubMed: 9741477]
14. Sato F, et al. Projections from the insular cortex to pain-receptive trigeminal caudal subnucleus (medullary dorsal horn) and other lower brainstem areas in rats. Neuroscience. 2013; 233:9–27. DOI: 10.1016/j.neuroscience.2012.12.024 [PubMed: 23270856]
15. Allen GV, Saper CB, Hurley KM, Cechetto DF. Organization of visceral and limbic connections in the insular cortex of the rat. J Comp Neurol. 1991; 311:1–16. DOI: 10.1002/cne.903110102 [PubMed: 1719041]
16. Yasui Y, Breder CD, Saper CB, Cechetto DF. Autonomic responses and efferent pathways from the insular cortex in the rat. J Comp Neurol. 1991; 303:355–374. DOI: 10.1002/cne.903030303 [PubMed: 2007654]
17. Knobloch HS, et al. Evoked axonal oxytocin release in the central amygdala attenuates fear response. Neuron. 2012; 73:553–566. DOI: 10.1016/j.neuron.2011.11.030 [PubMed: 22325206]
18. Dumais KM, Bredewold R, Mayer TE, Veenema AH. Sex differences in oxytocin receptor binding in forebrain regions: correlations with social interest in brain region- and sex- specific ways. Horm Behav. 2013; 64:693–701. DOI: 10.1016/j.yhbeh.2013.08.012 [PubMed: 24055336]
19. Donaldson ZR, Young LJ. Oxytocin, vasopressin, and the neurogenetics of sociality. Science. 2008; 322:900–904. DOI: 10.1126/science.1158668 [PubMed: 18988842]
20. Shamay-Tsoory SG, Abu-Akel A. The Social Salience Hypothesis of Oxytocin. Biol Psychiatry. 2016; 79:194–202. DOI: 10.1016/j.biopsych.2015.07.020 [PubMed: 26321019]
21. Burkett JP, et al. Oxytocin-dependent consolation behavior in rodents. Science. 2016; 351:375–378. DOI: 10.1126/science.aac4785 [PubMed: 26798013]
22. Aoki Y, et al. Oxytocin improves behavioural and neural deficits in inferring others' social emotions in autism. Brain. 2014; 137:3073–3086. DOI: 10.1093/brain/awu231 [PubMed: 25149412]
23. Scheele D, et al. An oxytocin-induced facilitation of neural and emotional responses to social touch correlates inversely with autism traits. Neuropsychopharmacology. 2014; 39:2078–2085. DOI: 10.1038/npp.2014.78 [PubMed: 24694924]
24. de Waal FBM, Preston SD. Mammalian empathy: behavioural manifestations and neural basis. Nat Rev Neurosci. 2017; 18:498–509. DOI: 10.1038/nrn.2017.72 [PubMed: 28655877]
25. Silberberg A, et al. Desire for social contact, not empathy, may explain "rescue" behavior in rats. Anim Cogn. 2014; 17:609–618. DOI: 10.1007/s10071-013-0692-1 [PubMed: 24126919]
26. Bullmore E, Sporns O. Complex brain networks: graph theoretical analysis of structural and functional systems. Nat Rev Neurosci. 2009; 10:186–198. DOI: 10.1038/nrn2575 [PubMed: 19190637]
27. Staub E. Helping a distressed person: Social, personality, and stimulus determinants. Advances in experimental social psychology. 1974
28. Spear LP. Adolescent alcohol exposure: Are there separable vulnerable periods within adolescence. Physiol Behav. 2015; 148:122–130. DOI: 10.1016/j.physbeh.2015.01.027 [PubMed: 25624108]
29. Brudzynski SM. Ethotransmission: communication of emotional states through ultrasonic vocalization in rats. Curr Opin Neurobiol. 2013; 23:310–317. DOI: 10.1016/j.conb.2013.01.014 [PubMed: 23375168]
30. Marlin BJ, Mitre M, D'amour JA, Chao MV, Froemke RC. Oxytocin enables maternal behaviour by balancing cortical inhibition. Nature. 2015; 520:499–504. DOI: 10.1038/nature14402 [PubMed: 25874674]
31. Gimpl G, Fahrenholz F. The oxytocin receptor system: structure, function, and regulation. Physiol Rev. 2001; 81:629–683. [PubMed: 11274341]

32. Power JD, Schlaggar BL, Lessov-Schlaggar CN, Petersen SE. Evidence for hubs in human functional brain networks. Neuron. 2013; 79:798–813. DOI: 10.1016/j.neuron.2013.07.035 [PubMed: 23972601]
33. Mikosz M, Nowak A, Werka T, Knapska E. Sex differences in social modulation of learning in rats. Sci Rep. 2015; 5:18114.doi: 10.1038/srep18114 [PubMed: 26655917]
34. Choe HK, et al. Oxytocin Mediates Entrainment of Sensory Stimuli to Social Cues of Opposing Valence. Neuron. 2015; 87:152–163. DOI: 10.1016/j.neuron.2015.06.022 [PubMed: 26139372]
35. Insel TR, Fernald RD. How the brain processes social information: searching for the social brain. Annu Rev Neurosci. 2004; 27:697–722. DOI: 10.1146/annurev.neuro.27.070203.144148 [PubMed: 15217348]
36. Valenta JG, Rigby MK. Discrimination of the odor of stressed rats. Science. 1968; 161:599–601. [PubMed: 5663306]
37. Sotocinal SG, et al. The Rat Grimace Scale: a partially automated method for quantifying pain in the laboratory rat via facial expressions. Mol Pain. 2011; 7:55.doi: 10.1186/1744-8069-7-55 [PubMed: 21801409]
38. Kiyokawa Y. Social Odors: Alarm Pheromones and Social Buffering. Curr Top Behav Neurosci. 2017; 30:47–65. DOI: 10.1007/7854_2015_406 [PubMed: 26602247]
39. Burgdorf J, et al. Ultrasonic vocalizations of rats (Rattus norvegicus) during mating, play, and aggression: Behavioral concomitants, relationship to reward, and self-administration of playback. J Comp Psychol. 2008; 122:357–367. DOI: 10.1037/a0012889 [PubMed: 19014259]
40. Oettl LL, Kelsch W. Oxytocin and Olfaction. Curr Top Behav Neurosci. 2017; doi: 10.1007/7854_2017_8
41. Langford DJ, et al. Social approach to pain in laboratory mice. Soc Neurosci. 2010; 5:163–170. DOI: 10.1080/17470910903216609 [PubMed: 19844845]
42. Ben-Ami Bartal I, Rodgers DA, Bernardez Sarria MS, Decety J, Mason P. Pro-social behavior in rats is modulated by social experience. Elife. 2014; 3:e01385.doi: 10.7554/eLife.01385 [PubMed: 24424411]
43. de Waal FB. Putting the altruism back into altruism: the evolution of empathy. Annu Rev Psychol. 2008; 59:279–300. DOI: 10.1146/annurev.psych.59.103006.093625 [PubMed: 17550343]
44. Moaddab M, Hyland BI, Brown CH. Oxytocin excites nucleus accumbens shell neurons in vivo. Mol Cell Neurosci. 2015; 68:323–330. DOI: 10.1016/j.mcn.2015.08.013 [PubMed: 26343002]
45. Adolphs R. The social brain: neural basis of social knowledge. Annu Rev Psychol. 2009; 60:693–716. DOI: 10.1146/annurev.psych.60.110707.163514 [PubMed: 18771388]
46. Bartz JA, Zaki J, Bolger N, Ochsner KN. Social effects of oxytocin in humans: context and person matter. Trends Cogn Sci. 2011; 15:301–309. DOI: 10.1016/j.tics.2011.05.002 [PubMed: 21696997]
47. Decety J, Moriguchi Y. The empathic brain and its dysfunction in psychiatric populations: implications for intervention across different clinical conditions. Biopsychosoc Med. 2007; 1:22.doi: 10.1186/1751-0759-1-22 [PubMed: 18021398]
48. Thioux M, Keysers C. Empathy: shared circuits and their dysfunctions. Dialogues Clin Neurosci. 2010; 12:546–552. [PubMed: 21319498]
49. LoParo D, Waldman ID. The oxytocin receptor gene (OXTR) is associated with autism spectrum disorder: a meta-analysis. Mol Psychiatry. 2015; 20:640–646. DOI: 10.1038/mp.2014.77 [PubMed: 25092245]
50. Skuse DH, et al. Common polymorphism in the oxytocin receptor gene (OXTR) is associated with human social recognition skills. Proc Natl Acad Sci U S A. 2014; 111:1987–1992. DOI: 10.1073/pnas.1302985111 [PubMed: 24367110]
51. Paxinos G, , Watson C. The rat brain atlas in stereotaxic coordinates 4. Academic Press; San Diego: 1998
52. Smith CJ, Wilkins KB, Mogavero JN, Veenema AH. Social Novelty Investigation in the Juvenile Rat: Modulation by the μ-Opioid System. J Neuroendocrinol. 2015; 27:752–764. DOI: 10.1111/jne.12301 [PubMed: 26212131]
53. Burkett JP, et al. Oxytocin-dependent consolation behavior in rodents. Science. 2016; 351:375–378. [PubMed: 26798013]

54. Christianson JP, et al. Safety signals mitigate the consequences of uncontrollable stress via a circuit involving the sensory insular cortex and bed nucleus of the stria terminalis. Biol Psychiatry. 2011; 70:458–464. DOI: 10.1016/j.biopsych.2011.04.004 [PubMed: 21684526]
55. Manning M, et al. Oxytocin and vasopressin agonists and antagonists as research tools and potential therapeutics. J Neuroendocrinol. 2012; 24:609–628. DOI: 10.1111/j.1365-2826.2012.02303.x [PubMed: 22375852]
56. Lukas M, Toth I, Veenema AH, Neumann ID. Oxytocin mediates rodent social memory within the lateral septum and the medial amygdala depending on the relevance of the social stimulus: male juvenile versus female adult conspecifics. Psychoneuroendocrinology. 2013; 38:916–926. DOI: 10.1016/j.psyneuen.2012.09.018 [PubMed: 23102690]
57. Tye KM, et al. Amygdala circuitry mediating reversible and bidirectional control of anxiety. Nature. 2011; 471:358–362. DOI: 10.1038/nature09820 [PubMed: 21389985]
58. Sidiropoulou K, et al. Dopamine modulates an mGluR5-mediated depolarization underlying prefrontal persistent activity. Nat Neurosci. 2009; 12:190–199. DOI: 10.1038/nn.2245 [PubMed: 19169252]
59. Dölen G, Darvishzadeh A, Huang KW, Malenka RC. Social reward requires coordinated activity of nucleus accumbens oxytocin and serotonin. Nature. 2013; 501:179–184. DOI: 10.1038/nature12518 [PubMed: 24025838]
60. Szot P, Bale TL, Dorsa DM. Distribution of messenger RNA for the vasopressin V1a receptor in the CNS of male and female rats. Brain Res Mol Brain Res. 1994; 24:1–10. [PubMed: 7968346]
61. Dumais KM, Veenema AH. Vasopressin and oxytocin receptor systems in the brain: Sex differences and sex-specific regulation of social behavior. Front Neuroendocrinol. 2015; doi: 10.1016/j.yfrne.2015.04.003
62. Varela JA, Wang J, Christianson JP, Maier SF, Cooper DC. Control over stress, but not stress per se increases prefrontal cortical pyramidal neuron excitability. J Neurosci. 2012; 32:12848–12853. DOI: 10.1523/JNEUROSCI.2669-12.2012 [PubMed: 22973008]
63. Turrigiano GG, Leslie KR, Desai NS, Rutherford LC, Nelson SB. Activity-dependent scaling of quantal amplitude in neocortical neurons. Nature. 1998; 391:892–896. DOI: 10.1038/36103 [PubMed: 9495341]
64. Gschwendt M, et al. Inhibition of protein kinase C mu by various inhibitors. Differentiation from protein kinase c isoenzymes. FEBS Lett. 1996; 392:77–80. [PubMed: 8772178]
65. Christianson JP, et al. The sensory insular cortex mediates the stress-buffering effects of safety signals but not behavioral control. J Neurosci. 2008; 28:13703–13711. DOI: 10.1523/JNEUROSCI.4270-08.2008 [PubMed: 19074043]
66. Vetere G, et al. Chemogenetic Interrogation of a Brain-wide Fear Memory Network in Mice. Neuron. 2017; 94:363–374.e4. DOI: 10.1016/j.neuron.2017.03.037 [PubMed: 28426969]
67. Wheeler AL, et al. Identification of a functional connectome for long-term fear memory in mice. PLoS Comput Biol. 2013; 9:e1002853.doi: 10.1371/journal.pcbi.1002853 [PubMed: 23300432]
68. Tanimizu T, et al. Functional Connectivity of Multiple Brain Regions Required for the Consolidation of Social Recognition Memory. J Neurosci. 2017; 37:4103–4116. DOI: 10.1523/JNEUROSCI.3451-16.2017 [PubMed: 28292834]
69. Teles MC, Almeida O, Lopes JS, Oliveira RF. Social interactions elicit rapid shifts in functional connectivity in the social decision-making network of zebrafish. Proc Biol Sci. 2015; 282:20151099.doi: 10.1098/rspb.2015.1099 [PubMed: 26423839]
70. Newman ME. Modularity and community structure in networks. Proc Natl Acad Sci U S A. 2006; 103:8577–8582. DOI: 10.1073/pnas.0601602103 [PubMed: 16723398]
71. Wickham H. ggplot2: Elegant graphics for data analysis Springer Publishing Company Springer-Verlag; New York: 2009
72. Briatte F. ggnet: Functions to plot networks with ggplot2. R package version 0.1.0. https://github.com/briatte/ggnet

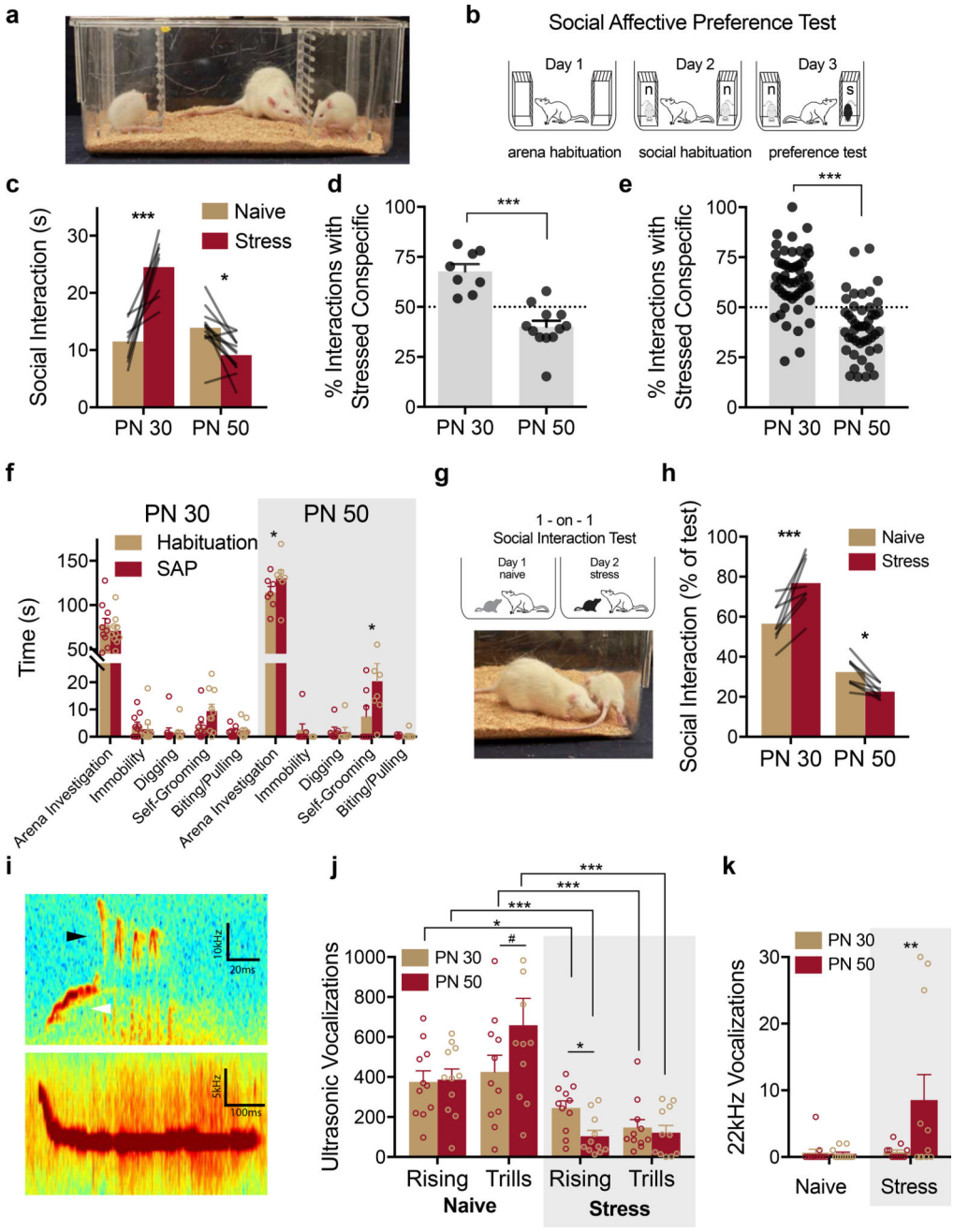

Figure 1. Social affective preference (SAP)

(A) The SAP arena containing juvenile conspecifics on the left and right with an experimental adult in the center. **(B)** Diagram of SAP test procedure. **(C)** Mean (individual replicates shown as connecting lines) time spent in social interaction with the naive or stressed conspecific by age (n = 8, PN 30; n = 12, PN 50). A bidirectional effect of age was apparent in time spent interacting with the stressed conspecifics ($F_{AGE}(1, 18) = 27.93$, $p < 0.0001$; $F_{AFFECT}(1, 18) = 9.965$, $p = 0.006$; $F_{AGE*AFFECT}(1, 18) = 46.05$, $p < 0.0001$). Experimental rats spent more time exploring the stressed PN 30 conspecific compared to the PN 30 naive, but spent less time exploring the stressed PN 50 conspecific compared to the

PN 50 naive. **(D)** Mean (+ SEM with individual replicates) data in C expressed as the percent of time spent interacting with the stressed conspecifics relative to the total time spent interacting. Experimental adults showed a marked preference (values greater than 50%) for interaction with stressed conspecifics and avoidance (values less than 50%) of stressed adults ($t(18) = 5.783$, $p < 0.0001$, 2-tailed). **(E)** Mean (+ SEM with individual replicates, $n = 51$ for PN 30, $n = 46$ for PN 50) percent preference for interacting with the stressed conspecific pooled from all of the subjects in the experimental control groups included in the current report including vehicle, sham, and light OFF control groups of the later experiments. Percent preference scores for PN 30 and PN 50 interactions were significantly different $t(95) = 7.66$, $p < 0.0001$, 2-tailed) from each other, and in both conditions the mean percent preference differed from 50% (PN 30: $t_{\text{one-sample}}(50) = 6.49$, $p < 0.0001$, 2-tailed; PN 50: $t_{\text{one-sample}}(45) = 4.39$, $p < 0.0001$, 2-tailed). **(F)** Mean (+ S.E.M. with individual replicates) time spent in non-social behaviors during habituation tests and SAP tests (n = 10, PN 30; n = 7 PN 50). More investigation of the arena and time spent self-grooming was observed in the PN 50 rats ($F_{\text{AGE*BEHAVIOR*TEST}}(4, 60) = 3.014$, p = 0.025). **(G)** Diagram of 1-on-1 social interaction test and photo of typical adult-initiated interactions. **(H)** Mean (individual replicates, ns = 8/ age) time interacting with the naive or stressed conspecific in a 1-on-1 test shown as percent of test time. Experimental adults spent significantly more time interacting with the stressed PN 30 conspecific but significantly less time with the stressed PN 50 conspecific compared to the respective naive conspecific targets ($F_{\text{AGE}}(1, 14)$ 103.10, $p < 0.0001$; $F_{\text{AGE*AFFECT}}(1, 14) = 31.34$, $p < 0.0001$). **(I)** Representative audio spectrograms depicting rising (top, white arrow), trills (top, black arrow) and 22kHz ultrasonic vocalizations (USVs). Scale bars indicate Y-axis ranges: 60–70kHz (top) and 30–35kHz (bottom). **(J–K)** Mean (+SEM with individual replicates, ns = 11/group) number of rising and trill USVs recorded during 5 min one-on-one social interactions. Fewer rising and trill calls were observed during interactions with stressed conspecifics with fewer rising calls observed in stressed adults compared to stressed juveniles than stressed juveniles ($F_{\text{STRESS}}(1, 40) = 26.16$, $p < 0.0001$; $F_{\text{CALL TYPE}}(2, 80) = 60.86$, $p < 0.0001$; $F_{\text{STRESS*CALL TYPE}}(2, 80) = 20.18$, $p < 0.0001$; $F_{\text{CALL TYPE*AGE}}(2, 80) = 3.43$, $p = 0.37$). *$p < 0.05$, ** $p < 0.01$, *** $p < 0.001$ (Sidak).

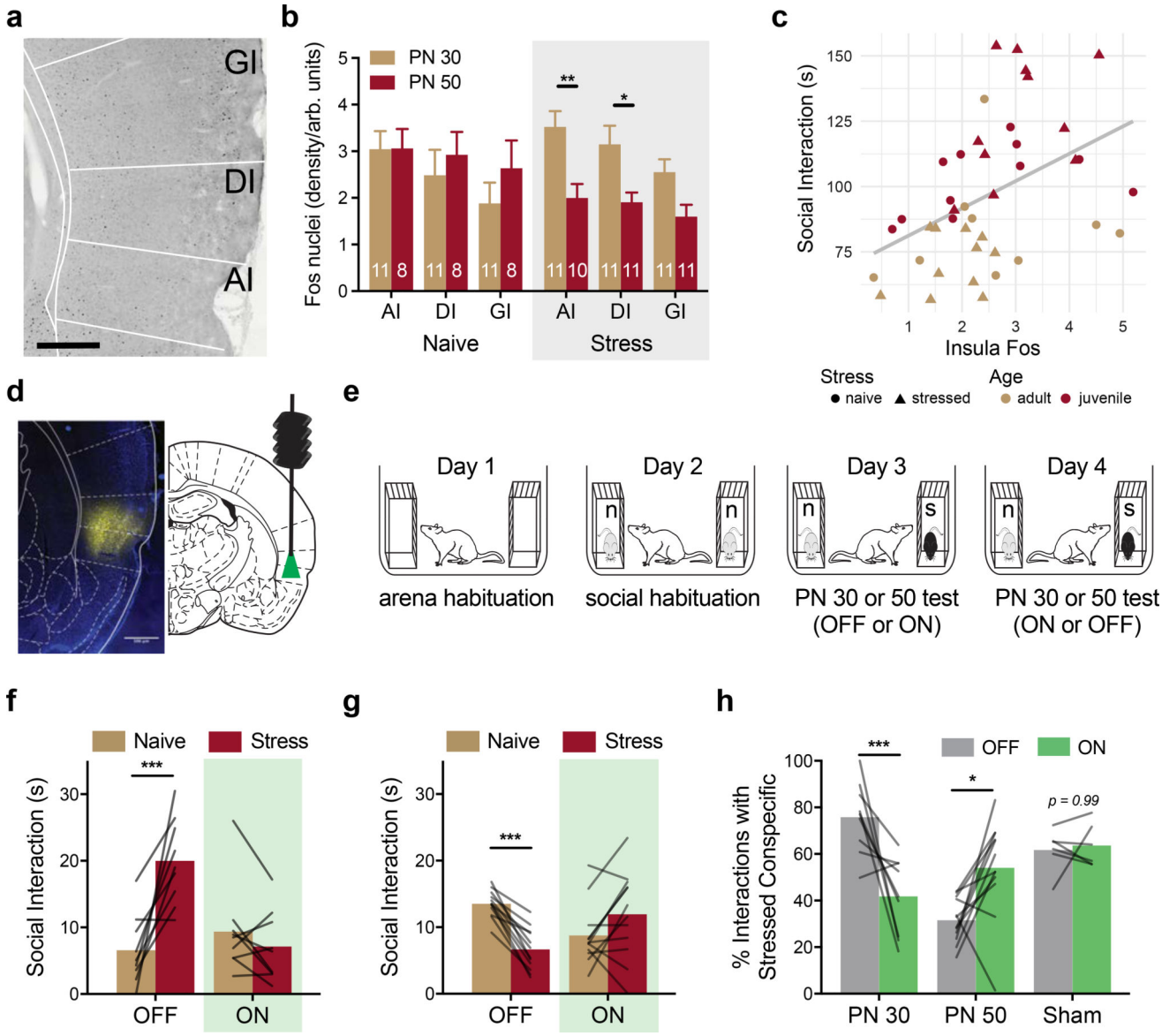

Figure 2. Optogenetic silencing of insular cortex during SAP tests

(A) Representative digital photomicrograph containing insular cortex regions and Fos immunoreactive nuclei (black ovoid particles). Scale bar = 500μm. **(B)** Mean (+SEM, numbers indicate number of replicates) Fos immunoreactive nuclei by insular cortex subregion (AI = Agranular, DI = Dysgranular, GI = Granular) quantified 90 min after social interaction with a naive PN 30, naive PN 50, stressed PN 30 or stressed PN 50 conspecific (5 min test). Fos was found in all regions, but there was an effect of stress for interactions with PN 50 rats, such that less Fos was evident after interaction with PN 50 stressed conspecific interactions than after interaction with PN 50 naive conspecifics, and there was less Fos in the AI and DI after interactions with PN 50 Stressed rats than after interactions with PN 30 stressed rats ($F_{\text{STRESS*AGE}}(1, 36) = 6.21$, $p = 0.017$; $F_{\text{SUBREGION}}(2, 72) = 7.90$, $p = 0.001$). **(C)** Mean Fos immunoreactivity (pooled across insula) predicted time spent in social interaction. Regression analysis indicated strong prediction of social interaction by Fos level,

Age, and modest interactions between Stress, Fos and Age ($F_{FOS}(1, 34) = 19.72$, $p < 0.0001$, $F_{AGE}(1, 34) = 36.93$, $p < 0.0001$; $F_{FOS*STRESS}(1, 34) = 3.97$, $p = 0.055$; $F_{STRESS*AGE}(1, 34) = 4.09$, $p = 0.051$). **(D)** Native mCherry expression in the insular cortex (false colored yellow) from a brain slice adjacent to one containing the cannula tract. (Scale bar = 500μm). **(E)** Diagram of SAP tests for optogenetic experiments. **(F)** Mean time spent interacting with PN 30 juvenile conspecifics (n = 9) or **(G)** PN 50 adult conspecifics (n = 12) on Days 3 and 4 of the SAP test. In the light OFF condition, the experimental adult spent significantly more time interacting with the stressed PN 30 conspecific, but this pattern was abolished in the light ON condition ($F_{AGE*STRESS*LIGHT}(1, 19) = 41.31$, $p < 0.0001$). In the light OFF condition, the experimental adult spent significantly less time interacting with the stressed PN 50 conspecific, but this pattern was reversed in the light ON condition. **(H)** Data from F and G converted to percent preference for interaction with stressed conspecifics. Here, a clear age by light interaction is apparent, with optogenetic silencing of insular cortex eliminating preference for interaction with the stressed juvenile and blocking the pattern of avoidance of stressed adult conspecifics ($F_{AGE*LIGHT}(1, 19) = 23.53$, $p = 0.0001$). No effect of optical stimulation was observed in sham transduced rats. * $p < 0.05$, ** $p < 0.01$, *** $p < 0.001$ (Sidak). Brain Atlas illustrations were reproduced with permission as previously published in *The Brain Atlas in Stereotaxic Coordinates*, 4th Edition, Paxinos, G. & Watson, C. Pages 296, 303, 306–317 & 332. Copyright Elsevier (1998).

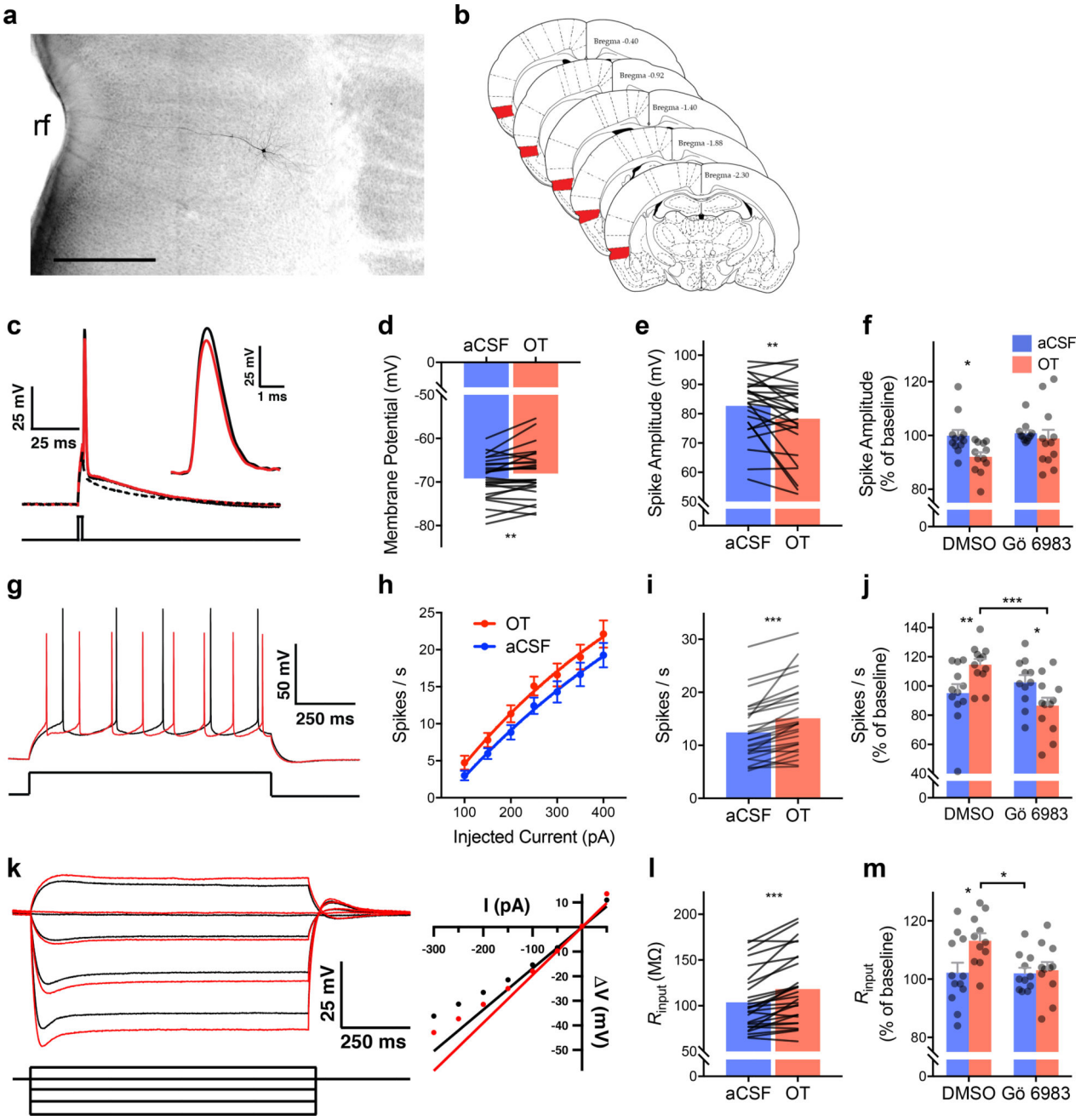

Figure 3. Intrinsic membrane properties in insular cortex pyramidal neurons are modulated by oxytocin and depend upon protein kinase C (PKC)

(A) Digital photomicrograph of a typical biocytin filled neuron, rf = rhinal fissure (Scale bar = 500μm). **(B)** Schematic diagram illustrating the region of interest for whole cell recordings (red shading). **(C)** Typical action potential before (black trace) and after bath application of 500nM OT (red). Inset: detail of the AP peak amplitude difference. Intrinsic properties were characterized from a sample of 27 neurons; the dependence of OT effects on PKC was determined by first characterizing the change in intrinsic properties from baseline followed by no treatment (aCSF) or OT (500nM) in either the presence of DMSO or DMSO and the

pan-PKC inhibitor Gö 6983 (200nM, aCSF-DMSO n = 12; OT-DMSO; n = 12, aCSF-Gö; n = 11; OT-Gö, n = 12). **(D)** Mean action potential amplitude; OT significantly reduced amplitude. **(E)** Mean resting membrane potential. OT significantly depolarized the membrane at rest. **(F)** Mean action potential amplitude (+S.E.M. with individual replicates); OT significantly reduced spike amplitude but did not change in the presence of Gö 6983 ($F_{OT}(1, 21) = 4.56$, $p = 0.044$, aCSF vs. OT, $p = 0.040$). **(G)** Typical train of spikes evoked by 1 s 150pA current injection before (black) and after (red) OT. **(H)** Mean (+/− SEM) spikes evoked by increasing current injections; OT increased the spike frequency ($F_{OT}(1, 279) = 10.42$, $p = 0.001$). **(I)** Mean action potentials evoked by 250pA current; significantly more spikes were evoked after OT. **(J)** Mean (+ S.E.M. and individual replicates) spike frequency upon 250pA depolarization; OT increased spiking compared to aCSF and Gö 6983 reduced spiking on its own ($F_{OT*Go}(1, 43) = 11.77$, $p = 0.0013$, aCSF-OT vs. Gö-OT, $p = 0.0007$). **(K)** Membrane potentials evoked by subthreshold and hyperpolarizing current injections (left) and typical rectification curve (right) before (black traces) and after (red traces) OT. **(L)** Mean input resistance (R_{input}); OT significantly increased R_{input}. **(M)** Mean (+ S.E.M. and individual replicates) input resistance. OT increased input resistance ($F_{Go}(2, 20) = 4.66$, $p = 0.043$, OT-DMSO vs. OT-Gö, $p = 0.03$). Symbols and connecting lines indicate individual replicates. *$p < 0.05$, ** $p < 0.01$, *** $p < 0.001$ (Sidak). Brain Atlas illustrations were reproduced with permission as previously published in *The Brain Atlas in Stereotaxic Coordinates*, 4th Edition, Paxinos, G. & Watson, C. Pages 296, 303, 306–317 & 332. Copyright Elsevier (1998).

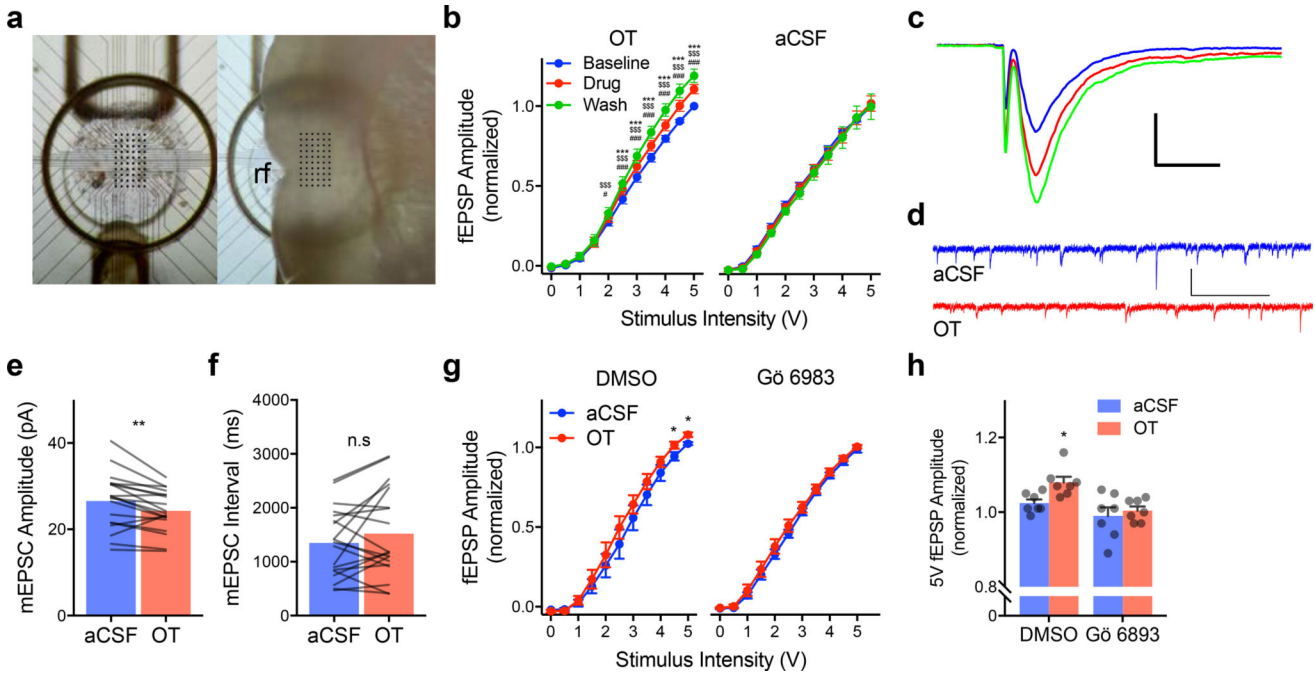

Figure 4. Oxytocin modulates excitatory synaptic transmission in the insular cortex

(A) Top view of 60 channel perforated MEA (left) for acute extracellular recordings of the insular cortex. Right depicts location of insular cortex slice during recording, rf = rhinal fissure. **(B)** Input/output curves for fEPSPs (Mean +/− SEM, OT n = 10, aCSF n = 9 slices) normalized to the peak amplitude observed in response to 5V stimulation under baseline conditions. OT significantly increased EPSP amplitude beginning at 2V with further enhancement during the washout ($F_{STIMULUS}(10, 90) = 598.20$, $p < 0.0001$; $F_{DRUG}(2, 18) = 11.99$, $p < 0.001$; $F_{STIMULUS*DRUG}(20, 180) = 11.34$, $p < 0.0001$). Without application of OT, EPSPs remain stable across the duration of the experiment (aCSF: $F_{STIMULUS}(10, 80) = 385.90$, $p < 0.0001$). ### $p < 0.0001$ OT vs. Baseline, $$$ $p < 0.0001$ Wash vs. Baseline, *** $p < 0.0001$ Wash vs. OT (Sidak). **(C)** Typical fEPSPs evoked by biphasic extracellular stimulation at baseline (blue) during application of 500nM OT (red) and after washout (green). Scale bar 500μV/ms. **(D)** Representative voltage clamp recordings of mEPSCs recorded before (aCSF; blue) and after OT (red). **(E)** Mean mEPSC amplitude before and after OT (n = 19 neurons); OT significantly reduced amplitude, **(paired $t(18) = 3.29$, $p = 0.004$, 2-tailed). **(F)** Mean mEPSC interval (n = 19 neurons); no effect of OT was apparent, (paired $t(18) = 1.42$, $p = 0.17$, 2-tailed). **(G)** Input/output curve for fEPSPs (Mean +/− S.E.M., n = 7 slices/condition) normalized to the peak amplitude observed in response to 5V stimulation under baseline conditions. OT (1μM) increased fEPSP at 4.5 and 5mV while no effect was observed in the presence of Gö 6983. *$F_{STIMULUS*DRUG}(10, 240) = 3.40$, $p < 0.0003$, OT vs. aCSF at 4.5 and 5V, $p = 0.0306$ and $p = 0.0181$, respectively (Sidak). **(H)** Mean (+ S.E.M. and individual replicates) fEPSP amplitude from (G) at 5V ($F_{OT}(1, 24) = 5.076$, $p = 0.034$). *OT-DMSO vs. aCSF-DMSO $p = 0.018$; vs. aCSF-Gö, $p = 0.002$; vs. OT-Gö, $p < 0.0004$ (Fisher's LSD).

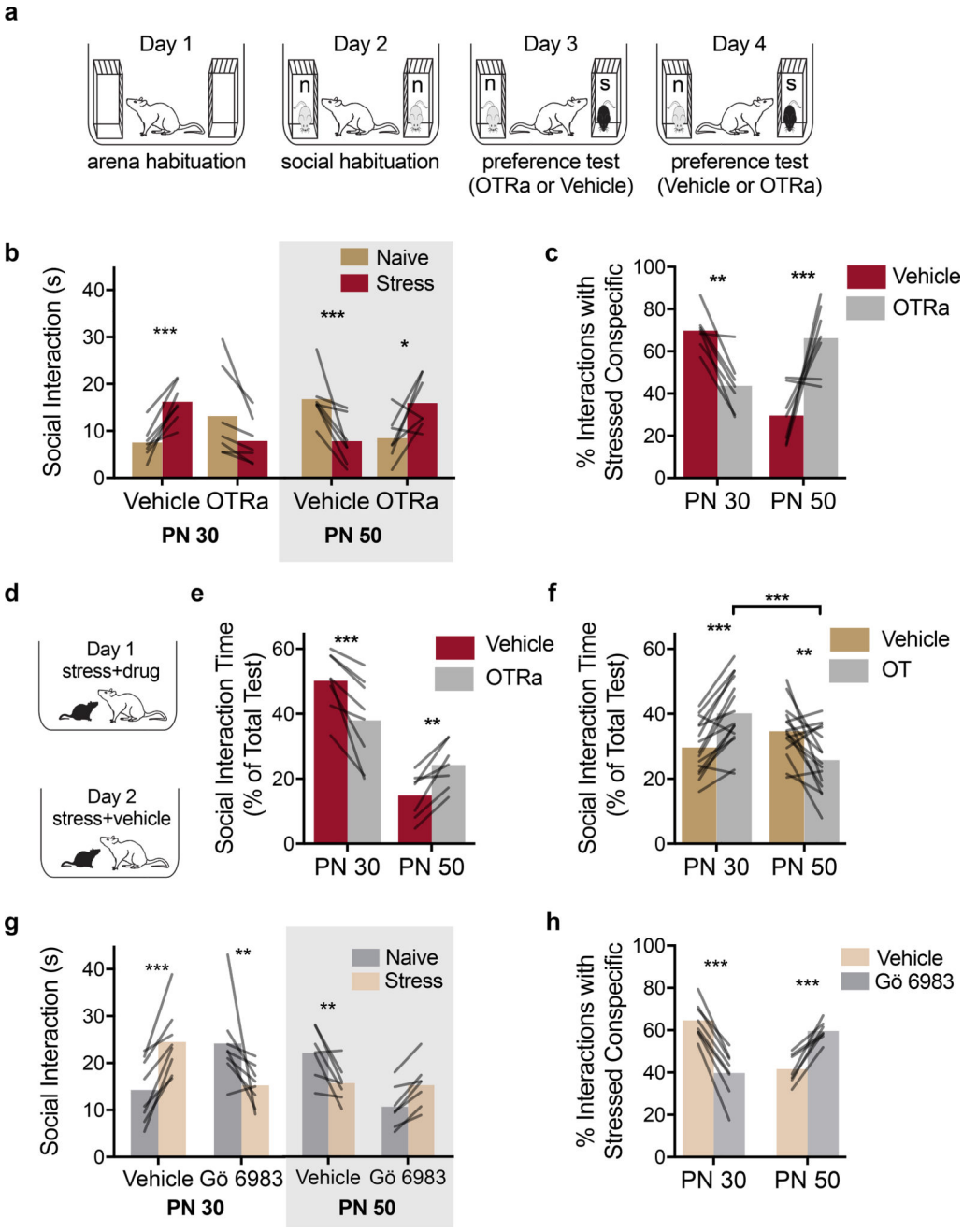

Figure 5. Social affective behaviors require insular cortex oxytocin

(A) Diagram of experimental design. **(B)** Mean (individual replicates) time spent exploring either PN 30 (n = 7) or PN 50 (n=7) conspecifics after bilateral intra-insula infusion of a selective OTR antagonist (OTRa, 20ng/side) in the SAP test. Vehicle-treated experimental adult rats spent more time interacting with the stressed than with the naïve PN 30 juvenile conspecifics and less time with the stressed than with the naïve PN 50 adult conspecifics. These effects were blocked and reversed, respectively, by infusion of OTRa ($F_{AGE*DRUG*STRESS}(1, 12) = 31.843$, $p = 0.0001$). **(C)** Data in (B) expressed as percent preference for interaction with the stressed conspecific (Mean with individual replicates).

OTRa significantly reduced preference for the stressed PN 30 while increasing time spent with the stressed PN 50 conspecific ($F_{AGE*DRUG}(1, 12) = 26.38$, $p < 0.0002$). **(D)** Diagram of 1-on-1 social interaction tests with stressed conspecifics and pretreatment with either vehicle or OTRa. **(E)** Mean (with individual replicates, normalized as percent of 3 to 5 min long test, time spent interacting with the stressed conspecific in a 1-on-1 test; PN 30: $n = 8$, PN 50: $n = 7$). OTRa significantly reduced time interacting with the stressed PN 30 conspecific but increased time interacting with the stressed PN 50 conspecific ($F_{AGE}(1, 13) = 28.66$, $p < 0.0001$; $F_{AGE*DRUG}(1, 13) = 32.56$, $p < 0.0001$). **(F)** Mean (with individual replicates) time spent interacting with a naive conspecific after intra insular cortex OT (250pg/side) or vehicle administration in a 1-on-1 social interaction (PN 30: $n = 15$; PN 50: $n = 15$). OT caused a significant increase in social interaction with naive PN 30 juveniles but a significant decrease in interaction with naive PN 50 adults ($F_{AGE*DRUG}(1, 28) = 30.08$, $p < 0.0001$). **(G)** Mean (individual replicates) time spent exploring either PN 30 (n = 8) or PN 50 (n = 7) conspecifics after intra-insula infusion of Gö 6983 (0.5uL/side 200nM) or vehicle (10% DMSO in water) in the SAP test. Vehicle-treated experimental adult rats spent more time interacting with the stressed than with the naïve PN 30 juvenile conspecifics and less time with the stressed than with the naïve PN 50 adult conspecifics. These trends were blocked and reversed, respectively, by the PKC inhibitor ($F_{STRESS*AGE*DRUG}(1, 13) = 63.75$, $p < 0.0001$). **(H)** Data in (G) expressed as percent preference for interaction with the stressed conspecific (Mean with individual replicates). Gö 6983 significantly reduced preference for the stressed PN 30 while increasing time spent with the stressed PN 50 conspecific ($F_{AGE*DRUG}(1, 13) = 141.10$, $p < 0.0001$). *$p < 0.05$, **$p < 0.01$, ***$p < 0.001$ (Sidak).

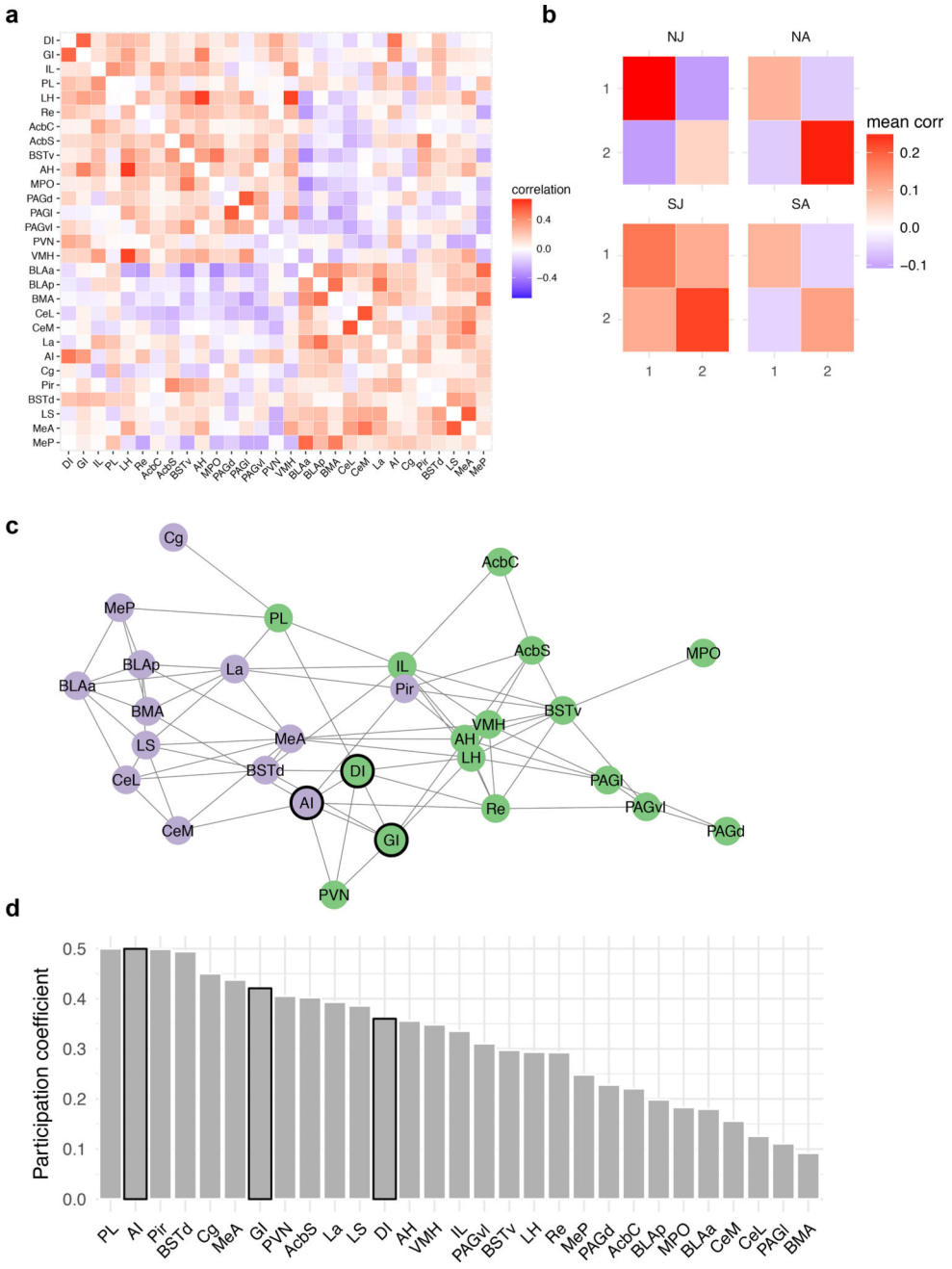

Figure 6. Insular Cortex and the Social Decision-Making Network

Fos immunoreactivity was determined in 29 ROIs of the rats (N=44) used in the USV quantification experiment (abbreviations provided in Sup. Table 1 and representative images in Sup. Fig. 7). **(A)** Correlation matrix indicating functional correlations (Kendall's tau) among ROIs. **(B)** Graph theory based community detection analyses identified two modules. Functional correlations within and between modules 1 and 2 were averaged across ROIs and shown for each group. **(C)** Network visualization of the nodes in modules 1 (green) and 2 (purple). Here an arbitrary threshold of 0.2 was applied to facilitate network visualization, such that only edges exceeding the threshold are shown, but note that all network analyses

were based on the unthresholded network. Insular cortex nodes are outlined in black. **(D)** The degree to which each node is connected to multiple functional modules was estimated by computing the participation coefficient. Bars corresponding to insular cortex ROIs are outlined in black. Network analyses by treatment group provided in Sup. Fig. 8. NJ = naive juvenile, NA = naive adult, SJ = stressed juvenile, SA = stressed adult.

Table 1

Effects of 500nM OT on insular cortex pyramidal intrinsic membrane properties

Property	aCSF	500nM OT	t(26)	p-value
Active	*Mean(SEM)*	*Mean(SEM)*		
AP threshold (mV)	−41.39 (0.83)	−41.89 (1.06)	0.893	*0.380*
Rheobase (pA)	1507 (85.5)	1429 (81.4)	3.217	****0.004***
Rise Rate (mV/ms)	225.4(13.04)	206.9 (13.42)	2.454	***0.021***
Spike Amplitude (mV)	82.72 (1.95)	78.31(2.46)	2.846	****0.009***
Spike Width (ms)	1.13 (0.05)	1.20 (0.06)	2.487	***0.020***
Decay rate (mV/ms)	−84.52 (3.16)	−77.93 (3.54)	3.471	****0.002***
ADP (mV)	11.40 (0.84)	11.60 (0.91)	0.664	*0.512*
Passive				
Resting potential (mV)	−69.2 (0.9)	−68.1 (1.1)	2.705	***0.012***
Time Constant (mV)	25.74(0.51)	23.81(0.68)	2.947	****0.007***
Input Resistance (MΩ)	103.7(6.23)	118.3(7.46)	5.473	*****<0.001***
Rectification Ratio	0.812(0.015)	0.824(0.015)	1.575	*0.127*
Sag (mV)	1.43(0.22)	1.10(0.15)	2.342	***0.027***
sAHP (mV × ms)	−320.3(36.13)	−230.6(31.49)	3.336	****0.003***

N = 27 cells;

* p < 0.05,

** p < 0.01,

*** p< 0.001